International Journal of Heat and Fluid Flow 30 (2009) 886–901

Contents lists available at ScienceDirect

International Journal of Heat and Fluid Flow

journal homepage: www.elsevier.com/locate/ijhff

Fluid flow due to combined convection in lid-driven enclosure having a circular body

Hakan F. Oztop [a,*], Zepu Zhao [b], Bo Yu [b]

[a] Dept. Mechanical Engineering, Fırat University, TR-23119 Elazig, Turkey
[b] Beijing Key Laboratory of Urban Oil and Gas Distribution Technology, China University of Petroleum (Beijing), Beijing 102249, PR China

ARTICLE INFO

Article history:
Received 1 July 2008
Received in revised form 24 March 2009
Accepted 23 April 2009
Available online 24 May 2009

Keywords:
Mixed convection
Enclosures
Lid-driven cavity
Inserted body

ABSTRACT

The present work is aimed to study mixed convection heat transfer characteristics for a lid-driven air flow within a square enclosure having a circular body. Flows are driven by the left lid, which slides in its own plane constant velocity. This wall is isothermal and it moves up or down in y direction while the other walls remain stationary. The horizontal walls are adiabatic. The cavity is differentially heated and the left wall is maintained at a higher temperature than the right wall. Three different temperature boundary conditions were applied for the inner cylinder as adiabatic, isothermal or conductive. The computation is carried out for wide ranges of Richardson numbers, diameter of inner cylinder and center and location of the inner cylinder. It was found that the most effective parameter on flow field and temperature distribution is the orientation of the moving lid. The circular body can be a control parameter for heat and fluid flow. An interesting obtained result that the thermal conductivity becomes insignificant for small values of diameter of the circular body.

1. Introduction

The lid-driven cavity flow has been a topic of great interest since it is frequently encountered in engineering applications. These applications include cooling of electronic equipments, drying or geophysics studies. These are listed in the study of Shankar and Despande (2000), Sharif (2007), Oztop and Dagtekin (2004). It is also an important problem in applied mathematical science to obtain benchmark result from written codes as given Mansutti et al. (1991), Ghia et al. (1982) and Bruneau and Saad (2006).

Ghia et al. (1982) used the driven flows in a square cavity as a model problem to study the effectiveness of the coupled strongly implicit multigrid (CSI-MG) method in the determination of high-Re fine-mesh flow solutions. Aydın (1999) showed the aiding and opposing mechanisms of mixed convection in a lid-driven cavity with moving vertical wall. He categorized the results for three flow regimes as the forced convection ($Ri \ll 1$), the mixed convection ($0.1 \leqslant Ri \leqslant 10$) and the natural convection ($Ri \gg 1$). Moallemi and Jang (1992) numerically studied mixed convective flow in a bottom heated square driven cavity and investigated the effect of Prandtl number on heat transfer. They observed that the effects of buoyancy are more pronounced for higher values of Prandtl number. Torrance et al. (1972), Iwatsu et al. (1993), Iwatsu and Hyun (1992), Mohammad and Viskanta (1993), Iwatsu and Hyun (1995) and Chamkha (2002) investigated the heat and fluid flow in lid-driven enclosures.

Convective heat transfer in cavities or channels can be controlled by inserting a body. The technique is mostly used to enhance the heat transfer using passive methods. There are many studies on natural convection in an enclosure with circular body in the literature Dong and Li (2004), Cesini et al. (1999), Kim et al. (2007), Jami et al. (2007) and Angeli et al. (2008).

Studies on mixed convection in lid-driven enclosures and natural convection in circular body inserted enclosures are cited up to this point. As seen from the literature that mixed convection in lid-driven enclosures with circular body insertion at different thermal boundary conditions is not accounted in these studies. However, control of flow fields and temperature distribution can be obtained by a circular body in lid-driven enclosures.

Literature on body inserted lid-driven enclosure is sparse. Mansutti et al. (1991) used the lid-driven flow in a square annulus as a benchmark problem to show the validity of the Discrete Vector Potential Model. They showed that the presence of inner square body inside the enclosure produces a secondary recirculating region in the part of the annulus with sliding wall. For increasing values of the Reynolds number, the circulation is convected away from the original symmetrical position at Re = 400 and it remains confined in a region close to the inner boundary for the larger values of Reynolds number. Dagtekin and Oztop (2002) inserted an isothermally heated rectangular block in a lid-driven cavity at different positions to simulate the cooling of electronic equipments. They found that dimension of the body is the most effective param-

* Corresponding author. Tel.: +90 424 237 0000x5328; fax: +90 424 241 5526.
E-mail addresses: hfoztop1@mail.com, hfoztop1@yahoo.com (H.F. Oztop).

0142-727X/$ - see front matter © 2009 Elsevier Inc. All rights reserved.
doi:10.1016/j.ijheatfluidflow.2009.04.009

Nomenclature

A	aspect ratio
c	center of location of the circular body
C_p	specific heat
D	diameter
Gr	Grashof number
H	height of the cavity
K	thermal conductivity ratio
L	length of the cavity
n	any direction
Nu	Nusselt number
P	Pressure
Pr	Prandtl number
R	radius
Re	Reynolds number
Ri	Richardson number
T	temperature
T_0	characteristic temperature
T_h	temperature of the hot wall
T_c	temperature of the cold wall
u, v	velocities
x, y	dimensional coordinates
X, Y	dimensionless coordinates

Greek letters

λ	thermal conductivity
ρ	density
υ	viscosity
β	thermal expansion coefficient

Subscripts

c	cold
h	hot

eter on mixed convection flow. Öztop and Dağtekin (2001) investigated the flow motion in a lid-driven enclosure with a rectangular body. In this case, the left vertical wall moves at constant speed. Oztop (2005) inserted a small rectangular body inside a lid-driven enclosure. Thus, different flow regimes can be investigated inside the enclosures as pouseuille and coutte flow. Shi and Khodadadi (2002, 2004, 2005) attached a moving fin onto the fixed vertical wall of the top-side moving enclosure to control unsteady flow and heat transfer. They showed that heat and fluid flow can be controlled using thin fin in lid-driven enclosures.

The main objective of the present study is to examine the effects of inserted circle shaped body into lid-driven enclosure on mixed convection heat transfer. We investigated the problem for three different thermal boundary conditions of inserted body as conductive, adiabatic and isothermal. Two different orientations ($+y$ and $-y$ directions) of the moving lid is studied to simulate the aiding and opposing flows. The above literature survey clearly shows that there is no study on mixed convection in a lid-driven cavity having a circle shaped body. Streamlines, isotherms, velocity profiles and Nusselt numbers will be present in next parts of the study for different Richardson numbers and thermal conductivity ratio values.

2. Model

The configuration is shown in Fig. 1a. The left side of the enclosure moves in $+y$ and $-y$ direction at constant velocity. It is a square enclosure (aspect ratio, $A = H/L = 1$). The temperature of moving wall is higher than that of right vertical wall and both of them are isothermal. Horizontal walls are insulated. A circle is inserted inside the enclosure with finite radius (R) and location of center of circle is shown by $c = c(x, y)$. The inserted body has three different temperature boundary conditions as isothermal, conductive or adiabatic. In this configuration, z-axis of the coordinate system coincides with the cylinders longitudinal axis, while the y-axis is parallel and opposed to the gravitational field. Thus, the cavity along z direction is assumed to prevail over L and the flow and temperature fields can be modeled as two-dimensional. Fig. 1b shows the detail of grid for steady-state predictions.

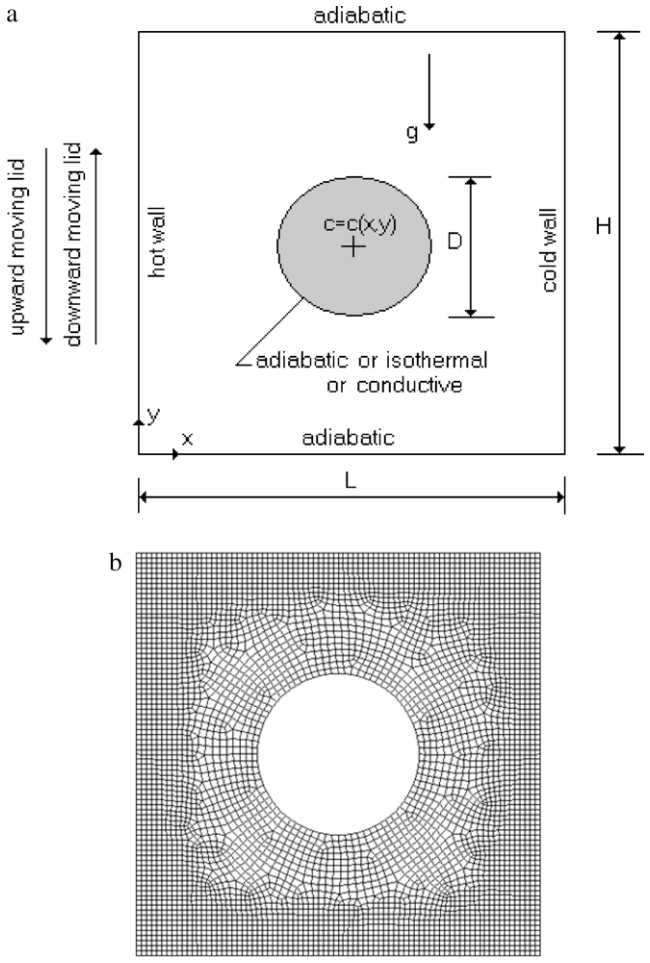

Fig. 1. (a) Schematical configuration of considered model with coordinates and boundary conditions, (b) grid distributions.

3. Theory

The equations describing the problem under consideration are based on the laws of mass, linear momentum and energy with buoyancy forces. Energy equation was written using Boussinesq approximation. It means that all physical properties of fluid are assumed to be constant except the density variation in body force term of the momentum equation. Radiation mode of heat transfer is neglected according to other modes of heat transfer. Viscous dissipation and pressure work are also neglected. Taking into consideration the above-mentioned assumptions, equations can write in dimensional form,

$$\frac{\partial u}{\partial x}+\frac{\partial v}{\partial y}=0 \tag{1}$$

$$u\frac{\partial u}{\partial x}+v\frac{\partial u}{\partial y}=-\frac{1}{\rho}\frac{\partial P}{\partial x}+\nu\left(\frac{\partial^2 u}{\partial x^2}+\frac{\partial^2 v}{\partial y^2}\right) \tag{2}$$

$$u\frac{\partial v}{\partial x}+v\frac{\partial v}{\partial y}=-\frac{1}{\rho}\frac{\partial P}{\partial y}+\nu\left(\frac{\partial^2 v}{\partial x^2}+\frac{\partial^2 v}{\partial y^2}\right)+g\rho\beta(T-T_C) \tag{3}$$

$$u\frac{\partial T}{\partial x}+v\frac{\partial T}{\partial y}=\frac{k}{\rho C_p}\left(\frac{\partial^2 T}{\partial x^2}+\frac{\partial^2 T}{\partial y^2}\right) \tag{4}$$

Reynolds, Prandtl, Grashof, Richardson numbers and dimensionless temperature, thermal conductivity ratio are given respectively by Eq. (5). The thermal conductivity ratio is defined with the ratio of thermal conductivity of air to solid.

$$\mathrm{Re}=\frac{V_p H}{\upsilon},\quad \mathrm{Pr}=\frac{\upsilon}{\alpha},\quad \mathrm{Gr}=\frac{g\beta(T_h-T_c)H^3}{\upsilon^2},\quad \mathrm{Ri}=\frac{\mathrm{Gr}}{\mathrm{Re}^2},$$
$$\theta=\frac{T-T_0}{T_h-T_c},\quad K=\frac{k_{air}}{k_{solid}}. \tag{5}$$

Velocities and pressure are

$$U=\frac{u}{V_p},\quad V=\frac{v}{V_p},\quad P=\frac{p}{\rho V_p^2}. \tag{6}$$

Dimensionless coordinates are

$$X=\frac{x}{L},\quad Y=\frac{y}{L}. \tag{7}$$

Heat conduction equation in solid part is given as

$$\left(\frac{\partial^2 T}{\partial x^2}+\frac{\partial^2 T}{\partial y^2}\right)=0 \tag{8}$$

Using the above parameters, the governing Eqs. (1)–(4) can be written in dimensionless form as

$$\frac{\partial U}{\partial X}+\frac{\partial V}{\partial Y}=0 \tag{9}$$

$$U\frac{\partial U}{\partial X}+V\frac{\partial U}{\partial Y}=-\frac{\partial P}{\partial X}+\frac{1}{\mathrm{Re}}\left(\frac{\partial^2 U}{\partial X^2}+\frac{\partial^2 U}{\partial Y^2}\right) \tag{10}$$

$$U\frac{\partial V}{\partial X}+V\frac{\partial V}{\partial Y}=-\frac{\partial P}{\partial Y}+\frac{1}{\mathrm{Re}}\left(\frac{\partial^2 V}{\partial X^2}+\frac{\partial^2 V}{\partial Y^2}\right)+\mathrm{Ri}\theta \tag{11}$$

$$U\frac{\partial \theta}{\partial X}+V\frac{\partial \theta}{\partial Y}=\frac{1}{\mathrm{RePr}}\left(\frac{\partial^2 \theta}{\partial X^2}+\frac{\partial^2 \theta}{\partial Y^2}\right) \tag{12}$$

$$\left(\frac{\partial^2 \theta}{\partial X^2}+\frac{\partial^2 \theta}{\partial Y^2}\right)=0 \tag{13}$$

Boundary conditions

Boundary conditions on the moving wall is

$$U=0,\quad V=1(\text{lid moves upward})\quad \text{or } V=-1(\text{lid moves downward}),\quad \theta=\theta_h \tag{14}$$

On the right wall;

$$U=V=0,\quad \theta=\theta_c \tag{15}$$

On top and bottom walls

$$U=V=0,\quad \frac{\partial \theta}{\partial Y}=0 \tag{16}$$

As we indicated above that we have three different thermal boundary conditions for circular body as

$$\text{For conductive, } \left(\frac{\partial \theta}{\partial n}\right)_{solid}=K\left(\frac{\partial \theta}{\partial n}\right)_{fluid} \tag{17}$$

$$\text{For isothermal, } \theta=0.5 \tag{18}$$

$$\text{For adiabatic, } \frac{\partial \theta}{\partial n}=0 \tag{19}$$

As well known from the literature that Richardson number is a measure of the relative strength of natural convection and forced convection for a chosen problem. Thus, Ri → 0, the heat transfer regime is forced convection and Ri → ∞, natural convection. When Ri ∼ 1 natural convection effects are comparable to the forced convection effects.

3.1. Numerical procedure

The solution of governing equations in Eqs. (1)–(4) is made by finite control volume technique. Thus, the equations are integrated over the control volume. Eq. (5) is also solved in the solid part of the cavity. This is two dimensional heat conduction equation. Then, algebraic equations were obtained. The SIMPLE method is used to couple the velocity and pressure term (Patankar, 1980). QUICK (Quadratic Upwind Interpolation for Convective Kinematics) scheme (Hayase et al., 1992) is performed for the discretization of convective terms in the momentum and energy equations. The calculations are done using the FLUENT (2002) version 6 commercial code. Conjugate boundary conditions can be found in any related paper as Varol et al. (2008).

3.2. Evaluation of Nusselt number

First of all, the result contains dimensionless velocities in x-and y-direction (u, v) and dimensionless Nusselt number both on left and right wall. The local Nusselt number along the wall is defined as

$$Nu_y=-\left(\frac{\partial \theta}{\partial X}\right)_w \tag{20}$$

The above equation defines convective heat flux along the cavity. The average Nusselt number is calculated by integrating as

$$\overline{\mathrm{Nu}}=\frac{1}{A}\int_0^1 \mathrm{Nu}_y dX \tag{21}$$

3.3. Grid independency and validation of the study

We presented the grid distribution for computational model in Fig. 1b. Grid independency test is important for this study due to complexity of the computational domain. We made also several test on grid independency by using different grid dimensions from 25 × 25 to 125 × 125. The results are obtained for mean Nusselt numbers at Re = 1000, Gr = 10^5, $c = c(x = 0.5, y = 0.5)$ and $R = 0.15$ and listed in Table 1. The table shows us that mean Nusselt numbers does not change for higher grid dimensions. Based on results from the table 100 × 100 grid dimensions were used in the present study.

Table 1
Grid independency check for Re = 1000, Gr = 10^5, $c = c$ ($x = 0.5$, $y = 0.5$) and $R = 0.15$.

Grid number	Mean Nu of hot wall	Mean Nu of cold wall
25 × 25	8.58	6.66
50 × 50	8.96	7.02
75 × 75	9.08	7.15
100 × 100	9.13	7.21
125 × 125	9.13	7.21

Table 2
Comparison of Nusselt number of present study with literature (a) Kahveci (2007) for Grid number 41 × 41, Ra = 10^6, X_p = 0.5, w = 0.1, k = 0.001 and (b) Iwatsu et al. (1993) for lid-driven cavity without any inserted body.

Nu_{max}	Partition wall	Cold wall
(a)		
Kahveci (2007)	1.63	1.94
Present	1.59	1.91
Ri	Iwatsu et al. (1993)	Present
(b)		
1.00	1.34	1.30
0.06	3.62	3.63
0.01	6.29	6.34

Validation tests were made with two different studies to compare obtained results with literature. In the first case, the computational procedure is validated against the numerical results of Iwatsu et al. (1993) and Sharif (2007) for a top heated moving lid and bottom cooled square cavity filled with air (Pr = 0.71). The general agreement between the present computation and those of Iwatsu et al. (1993) and Sharif (2007) are seen to be very well with a maximum difference within 5%. We also made a second test by comparing results with the partitioned enclosure for Rayleigh number, Ra = 10^6, thickness of the partition, w = 0.1 and, thermal conductivity ratio, K = 0.001. In the second case, we compared our result with Kahveci's study for tests, Kahveci (2007). In his case, conjugate–natural convection heat transfer and fluid flow has been performed for a fully partitioned square enclosure. Table 2 shows the comparisonal results for parameters of Grid number 41 × 41, Ra = 10^6 (by choosing Re ≅ 1), X_p = 0.5 (location of the partition), w = 0.1 (thickness of the partition) and (thermal conductivity ratio) K = 0.001. The table clearly indicates that obtained results

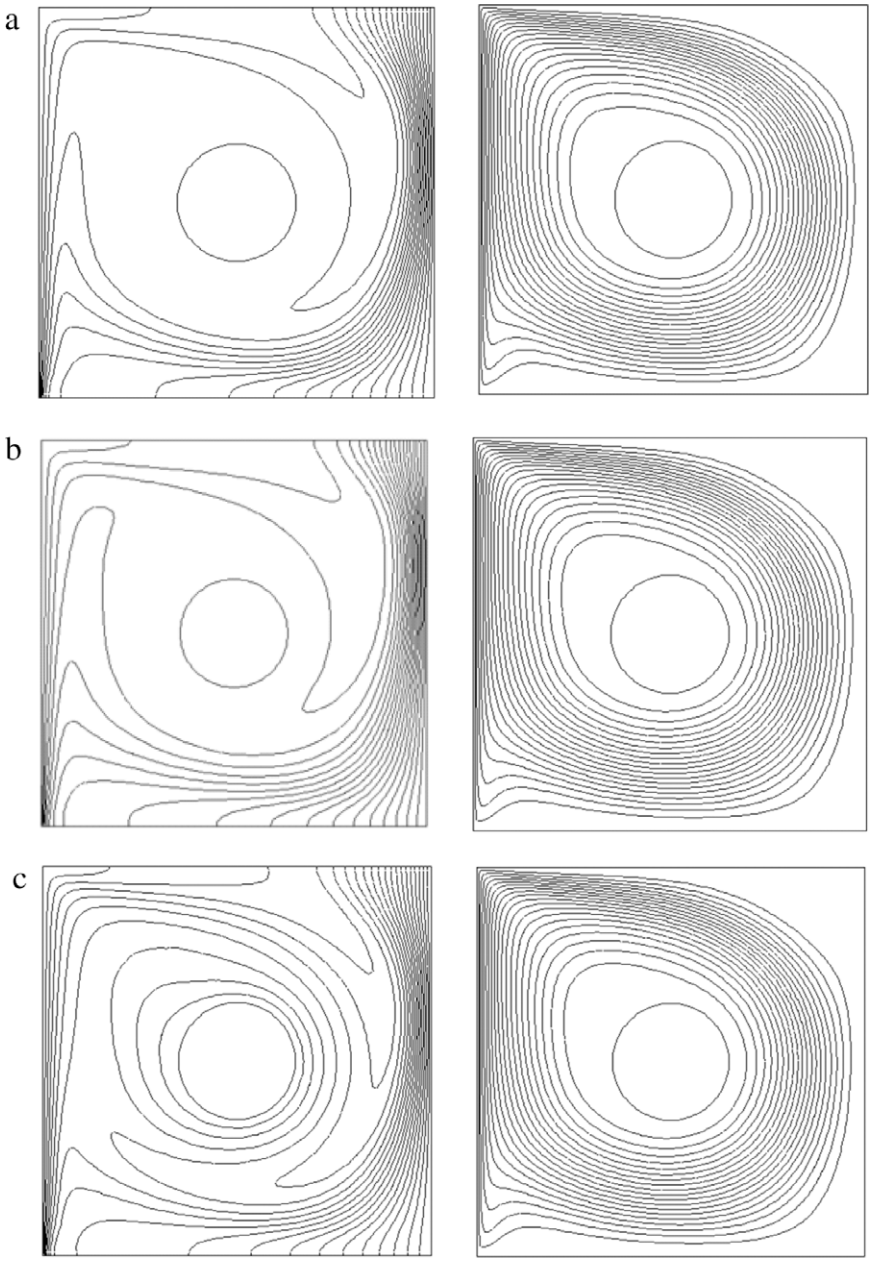

Fig. 2. Isotherms (on the left) and streamlines (on the right) in the case of upward moving left wall, (a) adiabatic, (b) conductive (K = 0.001) and (c) isothermal (θ = 0.5) for Gr = 10^5, Pr = 0.71, Re = 1000, c = 0.5 and R = 0.15.

of maximum Nusselt numbers are very close to Kahveci's result (2007) for both partition and cold walls.

4. Results and discussion

A numerical study on mixed convection heat transfer in a lid-driven cavity having a circular body was performed for different boundary conditions of the inserted circular body. The mixed convection phenomenon is influenced by three different thermal boundary conditions for the circular body as isothermal, conductive and adiabatic. We have also tested two orientations of the moving lid in $+y$ and $-y$ directions. Richardson number, location and dimension of the inserted circular body are other governing parameters which affect flow fields and temperature distribution. The value of thermal conductivity ratio for the case of conductive body changes from 0.0001 to 10. Air is chosen as the working fluid of which Prandtl number is 0.71. The effect of each parameter is illustrated in this section. Finally, 36 different cases were considered in order to see the effects of governing parameters.

Fig. 2 shows the isotherms (on the left) and streamlines (on the right) for different thermal boundary conditions at $R = 0.15$, $c = 0.5$, $\mathrm{Re} = 1000$ and $\mathrm{Gr} = 10^5$ ($\mathrm{Ri} = 0.1$). In this figure, the left wall moves in $+y$ direction. Thus, small amount of fluid is pulled up towards the left top corner due to drag force created by the motion of the left lid and it circulates around the circular body in clockwise direction. The high Re number refers to the low Ri number due to definition of Richardson number as $\mathrm{Ri} = \mathrm{Gr}/\mathrm{Re}^2$. It means that the forced convection heat transfer is dominant compared to other modes of heat transfer. The Richardson number is a measure to

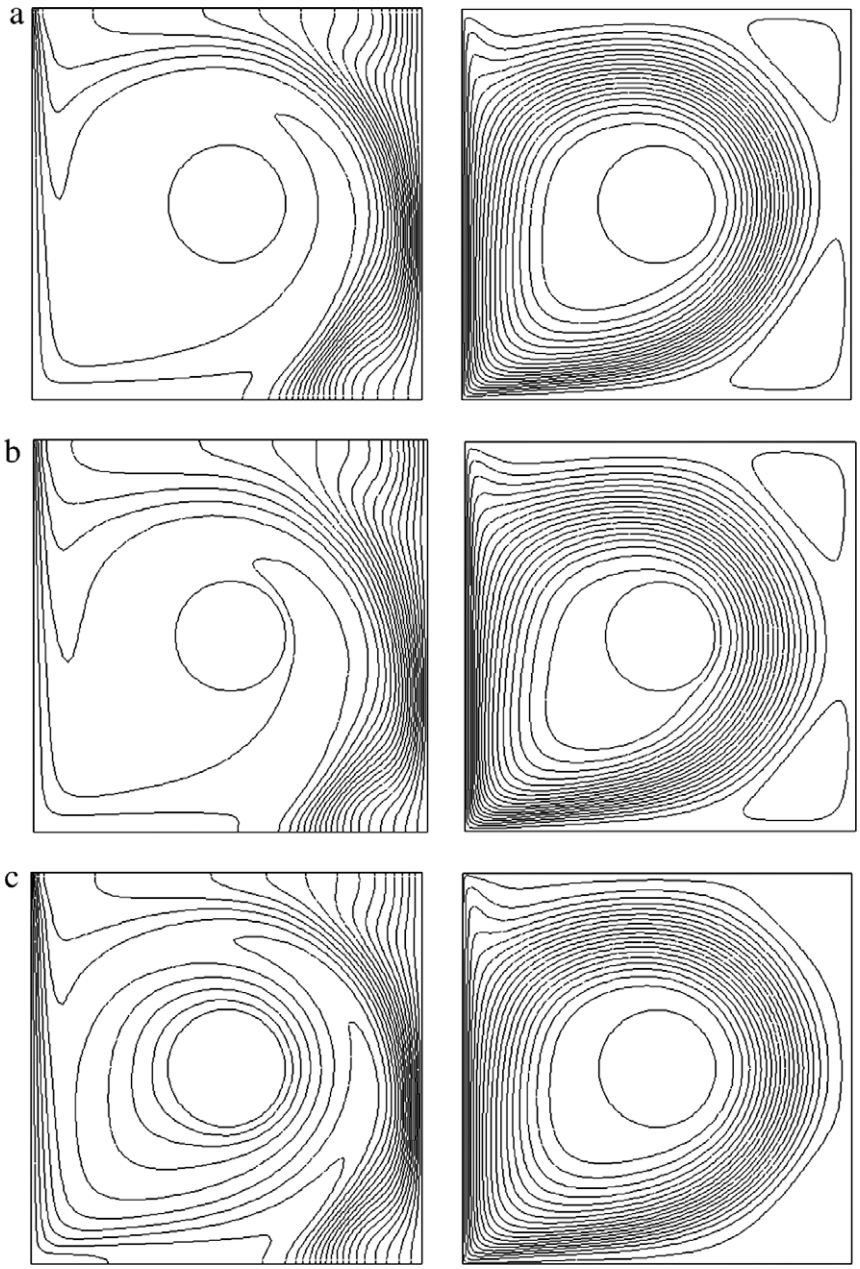

Fig. 3. Isotherms (on the left) and streamlines (on the right) in the case of downward moving left wall, (a) adiabatic, (b) conductive ($K = 0.001$) and (c) isothermal ($\theta = 0.5$) for $\mathrm{Gr} = 10^5$, $\mathrm{Pr} = 0.71$, $\mathrm{Re} = 1000$, $c = 0.5$ and $R = 0.15$.

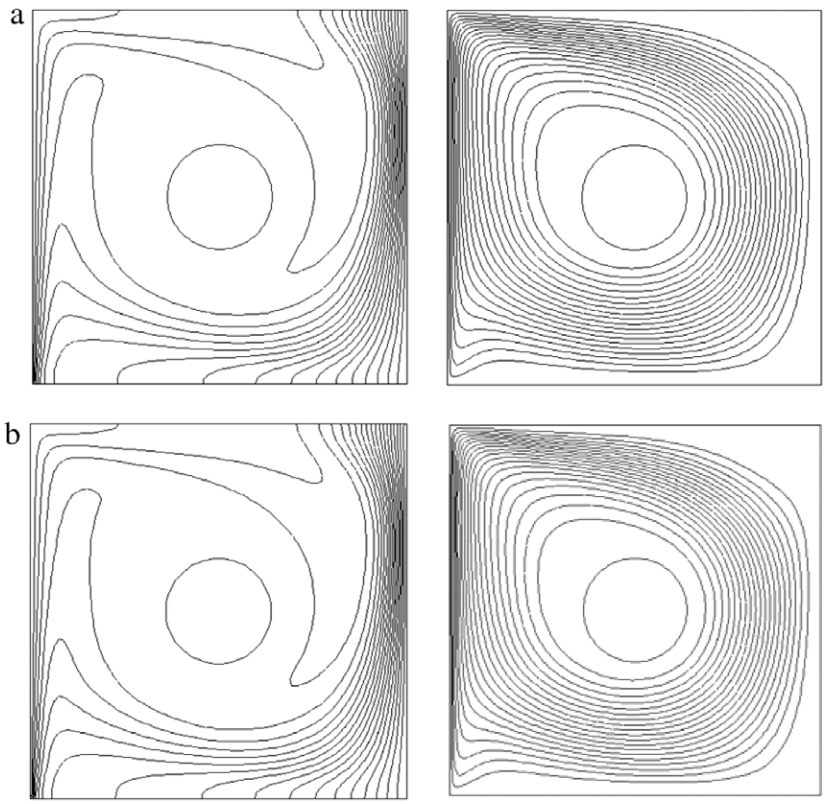

Fig. 4. Isotherms (on the left) and streamlines (on the right) in the case of upward moving left wall for $R = 0.15$, $Gr = 10^5$, $Pr = 0.71$, $c = 0.5$ and $Re = 1000$, (a) $K = 0.1$ and (b) $K = 1$.

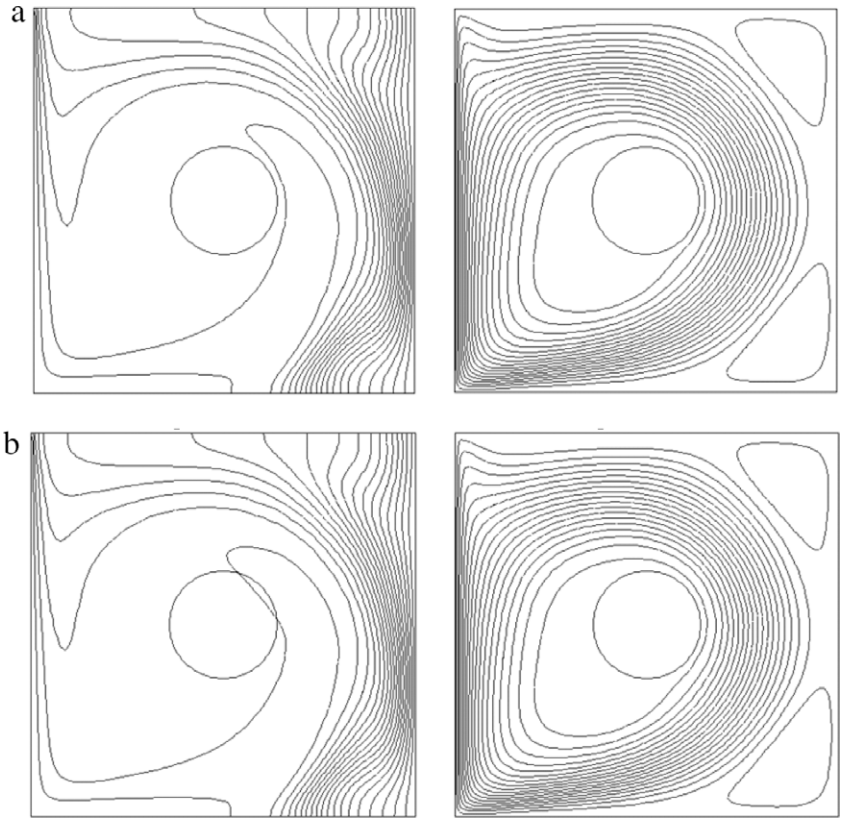

Fig. 5. Isotherms (on the left) and streamlines (on the right) in the case of downward moving left wall for $R = 0.15$, $Gr = 10^5$, $Pr = 0.71$, $c = 0.5$ and $Re = 1000$, (a) $K = 0.1$ and (b) $K = 1$.

define the regime of heat transfer as when $Ri \gg 1$ natural convection is dominant, $Ri = 1$ mixed convection heat transfer exists and $Ri \ll 1$ forced convection is dominant. In other words, limiting case $Ri \cong 0$ and $Ri \cong \infty$ correspond to the forced and natural convection flows, respectively. Fig. 2a and b present the streamlines and isotherms for the adiabatic and conductive body, respectively.

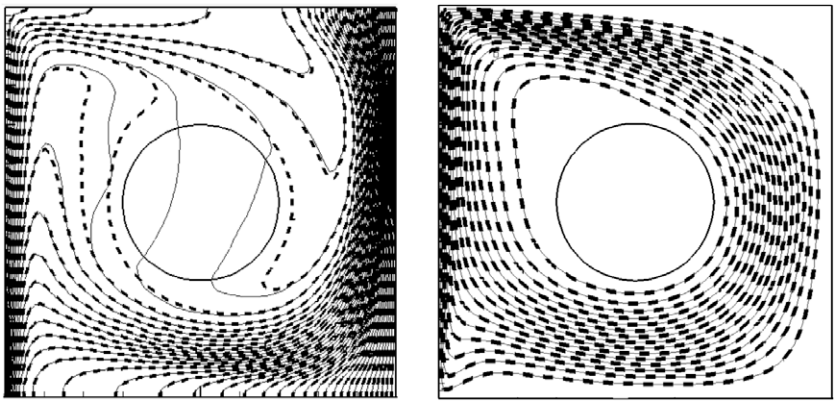

Fig. 6. Isotherms (on the left) and streamlines (on the right) in case of upward moving left wall for $R = 1000$, $Gr = 10^5$, $Pr = 0.71$, $c = 0.5$ and $Re = 1000$, Solid lines represent $K = 10$ and dashed lines represent $K = 0.001$.

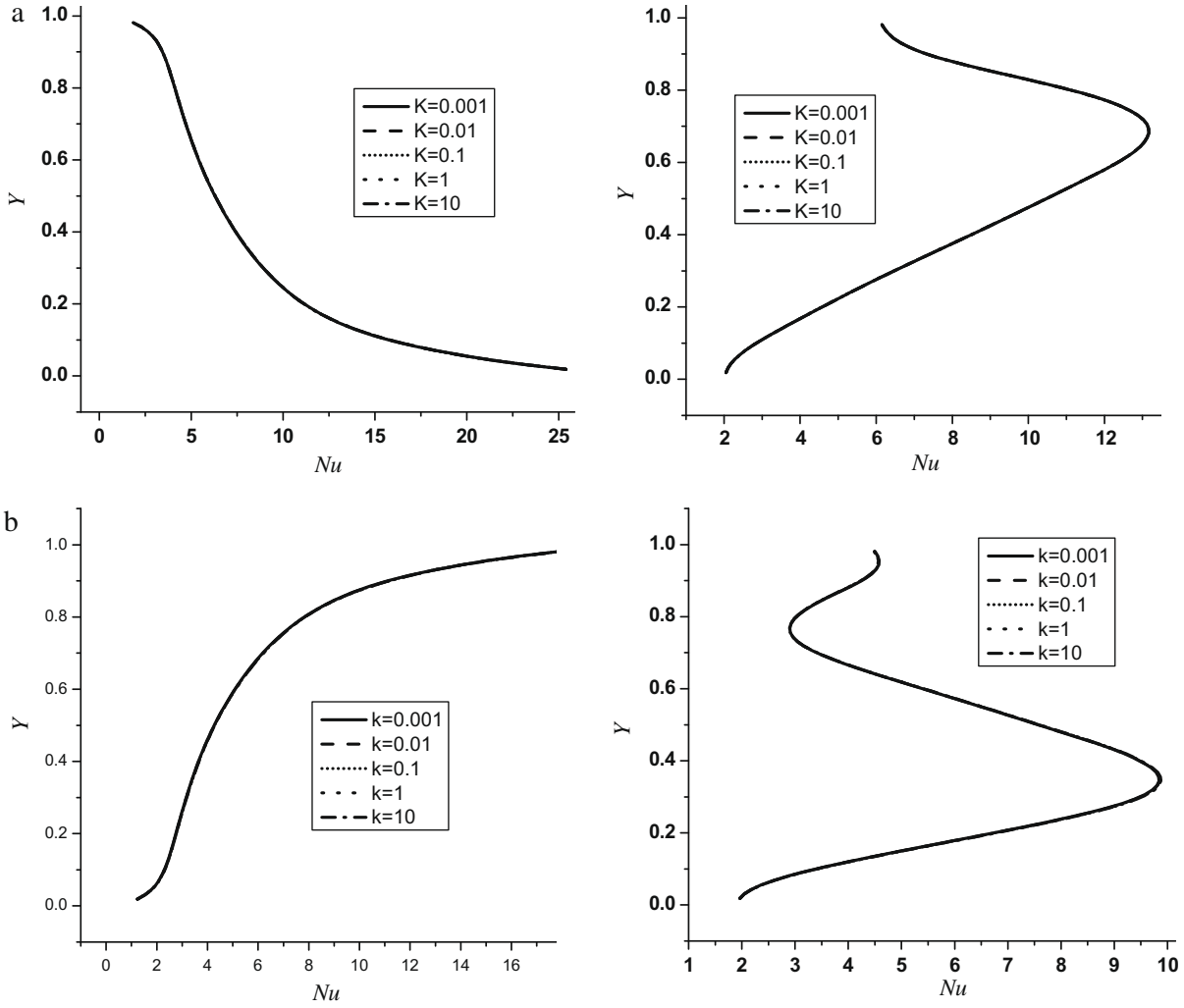

Fig. 7. Variation of local Nusselt numbers at different values of thermal conductivity ratio for hot wall (on the left column) and cold wall (on the right column) (a) hot wall moving upwards (on top row) and (b) hot wall moving downwards (on bottom row).

For these boundary conditions, both flow field and temperature distribution are almost same due to strong convection. The body behaves as barrier for the flow field but it is not an effective parameter on temperature field. In the case of isothermal boundary conditions, which are defined as neutral boundary conditions ($\theta = 0.5$), the isotherms are clustered near the circle and heated fluid moves towards to the left top corner. On the contrary, the flow field becomes identical with other cases due to the strongly dominant regime of forced convection. There are very small eddies at the right bottom and top corners but they are not presented on figure. Similarly, a small circulation is formed near the left bottom corner due to impinged circulation flow to the bottom wall. Fig. 3 displays the isotherms (on the left) and streamlines (on the right) for the same governing parameters of Fig. 2 except the orientation of moving lid. In this case, the lid moves downward ($-y$ direction), the flow impinges to the bottom horizontal wall and it turns in counterclockwise around the circular body. Two big cells are formed at the top and bottom right corners in clockwise rotating direction. The cells become smaller in the case of isothermal boundary conditions of body (Fig. 3b). There is a gap under the left side of the body. This gap has almost same size but it decreases for the isothermally heated circular body. In the case of moving lid in $-y$ direction, temperature distribution shows different configuration compared to the other boundary conditions of the inner body (Fig. 3c). In this case, there is thermal sink in the middle. Isotherms are circular around the source, a typical conductive feature. It seems to be appeared because of the interaction of new thermal source (not present in cases Fig. 3a and b) and thermal field to modify the situation. This is confirmed by the fact that the flow field is affected slightly. Fig. 4 illustrates the effects of thermal conductivity ratio on the temperature distribution and flow field for conductive circular body. The lid moves in $+y$ direction in this figure. Fig. 4a and b show the isotherms and streamlines for $K = 0.1$ and $K = 1$, respectively. In the case of $K = 1$, the body is less conductive and the

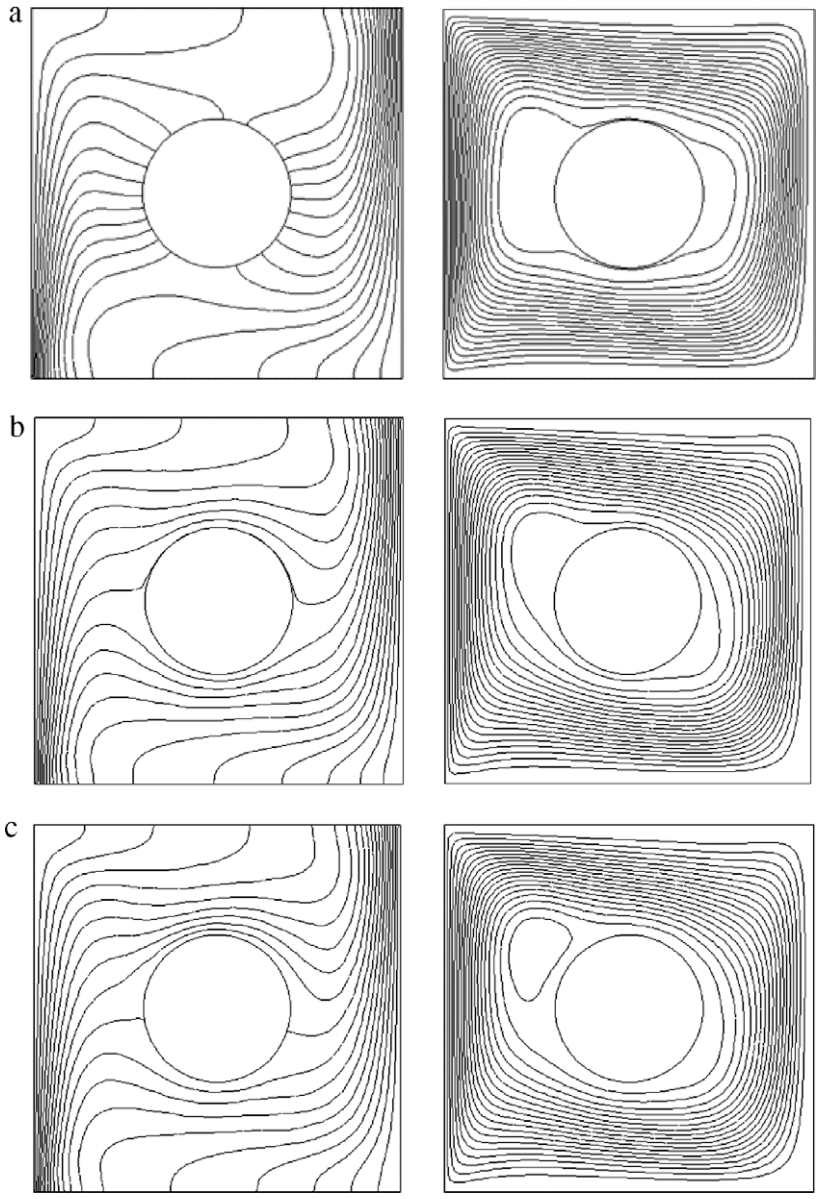

Fig. 8. Isotherms (on the left) and streamlines (on the right) in the case of upward moving wall, (a) adiabatic, (b) conductive ($K = 0.001$) and (c) isothermal ($\theta = 0.5$), Gr = 10^5, Pr = 0.71, $c = 0.5$, Re = 100 and $R = 0.2$.

temperature distribution of the body is less uniform and thus different temperature distribution is obtained than that of $K = 0.1$. Isotherms are clustered near the middle of the right wall and left bottom corner of the moving lid. As seen from the figure that dimensionless thermal conductivity ratio becomes insignificant on streamlines. Fig. 5 shows the isotherms and streamlines for the downward moving plate with same governing parameters of Fig. 4. In this case, the change of orientation of lid makes important effects on the streamlines and isotherms. But effects of thermal conductivity become very low. Nevertheless, the temperature distribution is affected from the thermal conductivity around the inserted body. A huge gap is formed near the left bottom side of the body due to direction of circulation of fluid caused by strong circulation in counterclockwise direction. The thermal conductivity ratio makes a small change on shape of this gap. Fig. 6. displays the isotherms and streamlines for upward moving case of $K = 10$ and $K = 0.001$. This figure is given to show the effects of thermal conductivity on solution. As seen from the figure, the solution is not sensitive to K value. This is because the insert body' s size is not large, the isotherms (especially in the regions near the vertical walls) and flow patterns are almost same for all K values. This is given by Fig. 6 to clarify that point. The variation of local Nusselt number along the hot (on the left) and cold walls (on the right) for different orientations are presented in Fig. 7a (hot wall moving upward) and Fig. 7b (hot wall moving downward), respectively. As seen from the figure, the trend of local Nusselt number changes with changing of orientation of moving wall. In other words, value of local Nusselt number decreases for upward moving wall and increases with downward moving lid. However, the local heat transfer increases around the upper side of middle part of cold wall due to presence of circle for upward moving lid. But the local Nusselt number has a peak around $y = 0.38$. Higher local Nusselt number values are obtained for upward moving lid. Fig. 8 shows the isotherms and streamlines for $R = 0.2$, $Gr = 10^5$ and $Re = 100$. In this

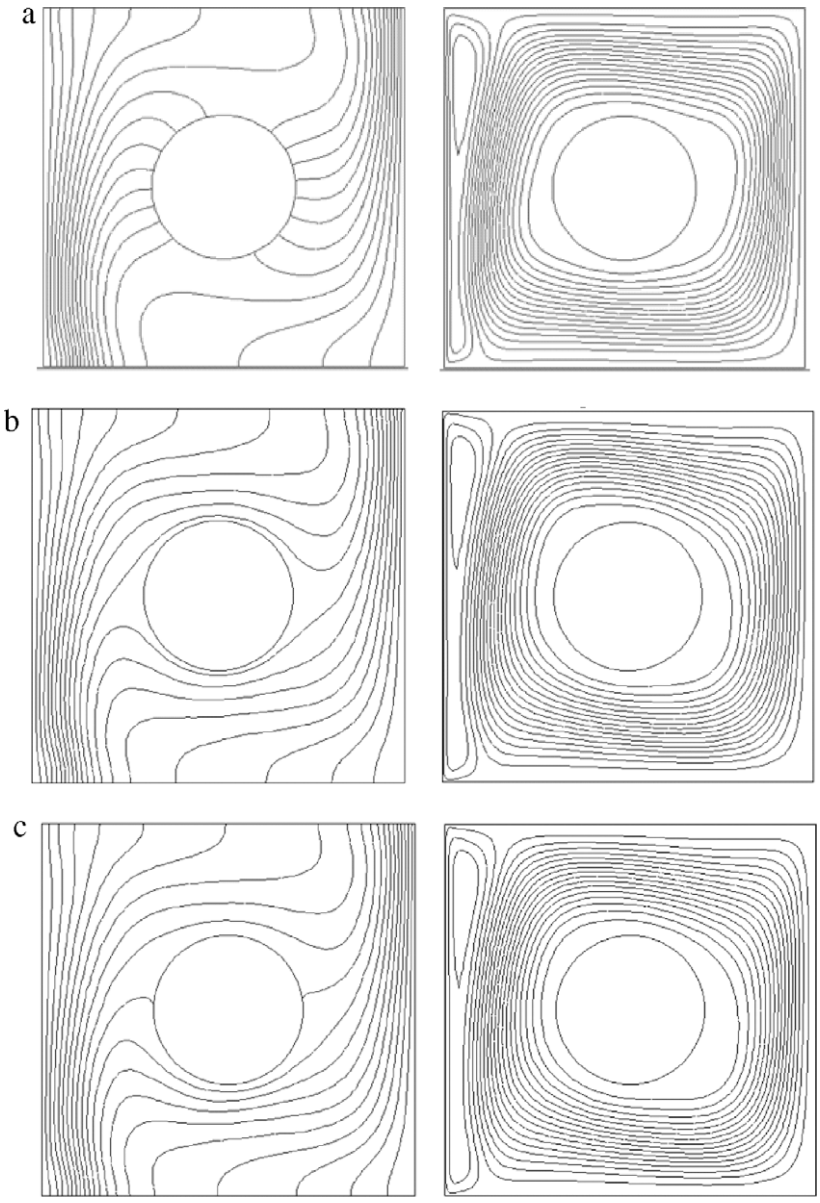

Fig. 9. Isotherms (on the left) and streamlines (on the right) in the case of downward moving wall, (a) adiabatic, (b) conductive ($K = 0.001$) and (c) isothermal ($\theta = 0.5$), $Gr = 10^5$ $Pr = 0.71$, $c = 0.5$, $Re = 100$ and $R = 0.2$.

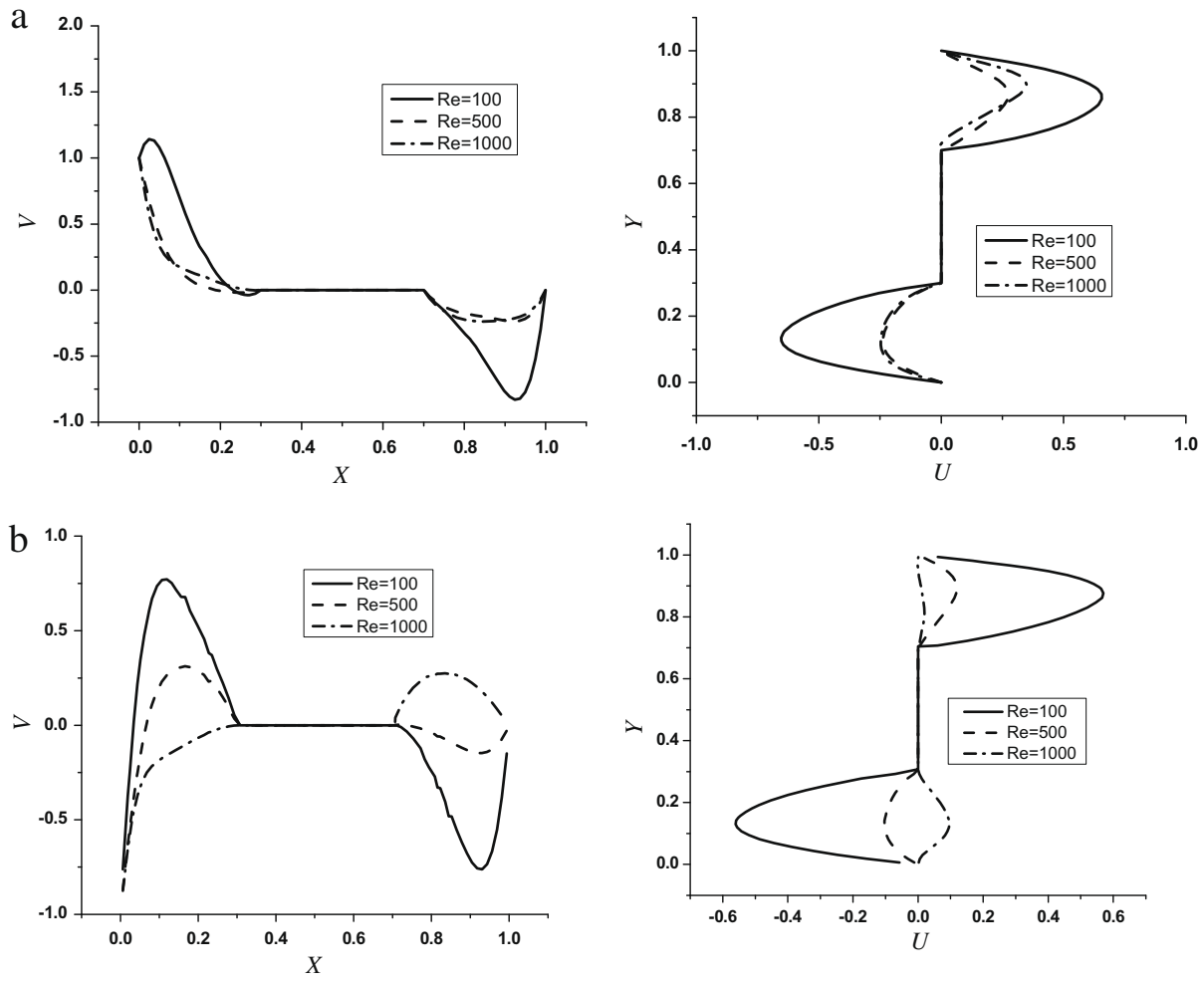

Fig. 10. Velocity profiles at the mid-section in y-axis (on the left) and x-axis (on the right) for different Reynolds number, (a) driving wall moves upwards and (b) driving wall moves downwards.

case, natural convection becomes dominant to forced convection. For the adiabatic boundary condition of inserted body, the body behaves as a barrier and an insulation material. Thus, the isotherms are attached to the body and streamlines are enlarged at the middle due to presence of the body. Two antisymmetric gaps are formed in left and side of the body due to moving lid. In case of conductive body, the left and right gaps move upward and downward of the body, respectively. Finally, a small recirculation is formed at the top side of the body with isothermal body. Fig. 9 presents the isotherms and streamline with the same parameters of Fig. 8 except direction of moving lid. In this figure, the left wall moves in $-y$ direction. For the all thermal boundary conditions of the circular body, a cell elongates near the moving lid. The center of this cell sits near the left top corner of the enclosure. The flow field around the circle is affected from the boundary conditions of the body. The isotherms are distributed around the body in isothermal and conductive cases.

Fig. 10a and b display the velocity profiles at the mid-section in y-axis (on the right column) and x-axis (on the left column) for different Reynolds number and different orientation of the moving lid. As seen from the figure, values of velocities are almost same for higher values of Reynolds number for upward moving wall. A parabolic velocity distribution is formed between inner body and insulated walls at the vertical mid-section of the enclosure as given in Fig. 10a (on the right). As seen from V-velocity profiles that values are decreased almost linearly from driving lid to body due to high flow velocity as given in Fig. 10a (on the left). It means that coutte-flow like regime is formed between lid and constant wall of the inner body. Fig. 11 presents the local Nusselt numbers along the cold walls (on the left column) and how wall (on the right column). In this figure, the top row belongs to upward moving lid and bottom row for downward moving lid. The local Nusselt number increases with the increase of Reynolds number in both walls. It has a maximum value around $y = 0.7$ on cold wall only when $Ri < 1$. It increases from the top to the bottom wall almost linearly due to decreasing of flow velocity. In the case of downward moving lid, the results are presented in Fig. 11b, the trend of local Nusselt number is completely different. S-shaped variation is formed for the higher Reynolds number and maximum heat transfer occurs at $y = 0.4$ on cold wall. Heat transfer increases from bottom to top and maximum heat transfer is formed as $Nu = 27$ at $y = 1$ due to moving of heated air from heated moving wall.

Fig. 12 shows the effects of diameter of circular body on temperature and fluid flow. In this figure, the results are given for upward moving lid and isothermal boundary conditions of the body at $Re = 1000$ and $Gr = 10^5$. The Fig. 12a shows the small gap is initiated near the top left side of the body for $R = 0.15$. With increasing of diameter of circular body, a secondary circulation is formed near the left top side of the body and its strength increases with increasing of circle diameter due to decreasing of the distance

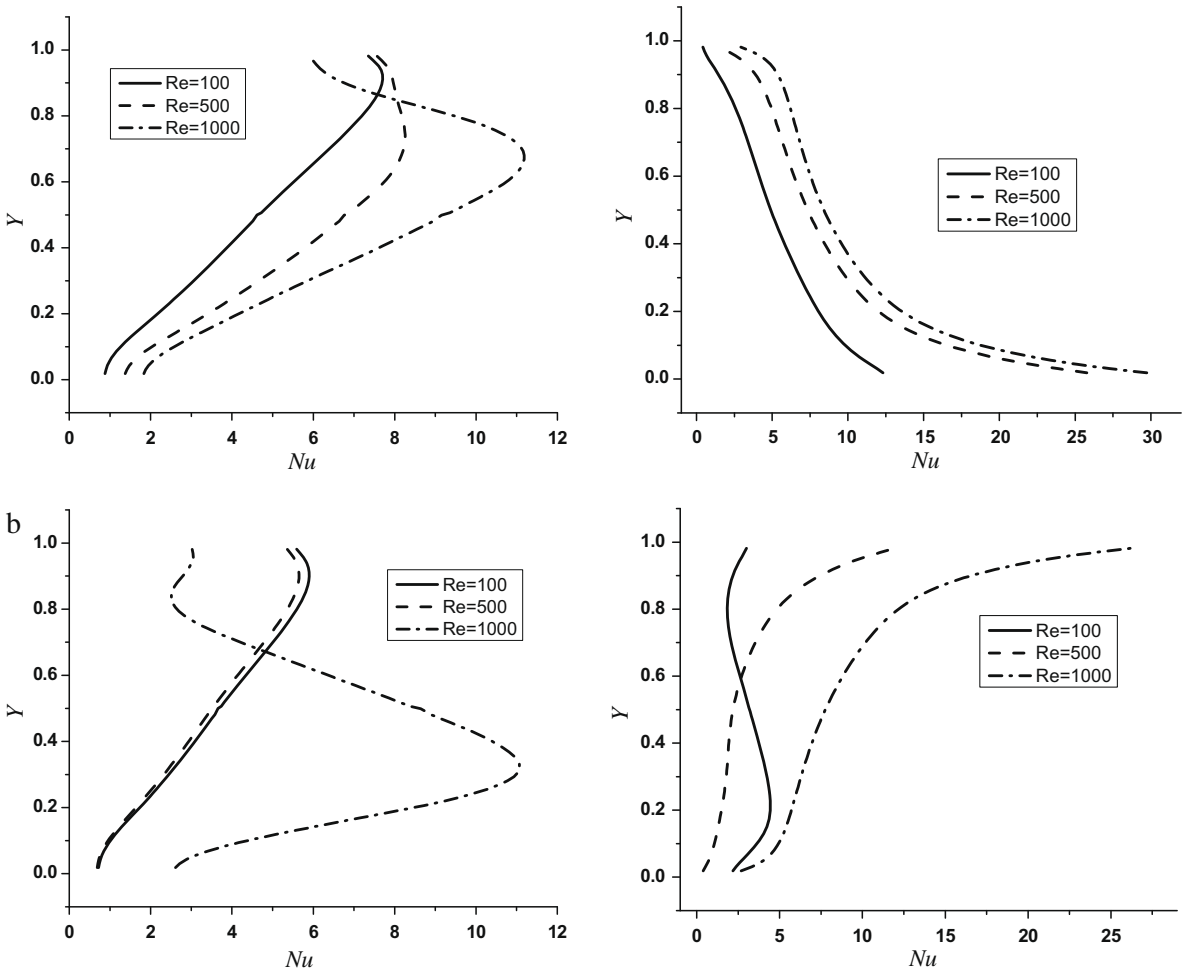

Fig. 11. Local Nusselt numbers along the cold walls (on the left) and hot wall (on the right) for different Reynolds numbers (a) driving wall moves upwards and (b) driving wall moves downwards.

between lid and body. Isotherms are cumulated near the left and right wall and thermal boundary layer and it becomes thinner with increasing of diameter of the body.

Fig. 13 is illustrated for different location of circular body. The location center is given by x and y coordinates of the center of body. Namely, middle located body is defined by $c = c(x = 0.5, y = 0.5)$. The detailed coordinate system is presented in Fig. 1a. When it locates near the top wall of the enclosure, the pulled flow impinged to the top wall and it flows between body and top wall. A small circulation cell is formed near the right top corner. Due to wide range between bottom wall and body, strength of flow decreases as seen from Fig. 13a. The isotherms are clustered near the top side of the circular body and heated flow moves through to the bottom sides from left side of the body. Double circulation cells are formed above the circular body. The impinged flow to the top wall deviates onto the circular body and it separates the flow into two parts. Thus, the isotherms are cumulated near the right bottom side of the right wall (Fig. 13b). For the location center of the circular body of $x = 0.4$ and $y = 0.5$, a cell was formed above the body and it moves through to the right side of the body. Flow velocity is very high between upward moving lid and circular body due to small gap. A mini circulation cell was formed at the right top corner but it is not showed in figure. Parallel isotherms are located around the body and they are cumulated near the right wall. When the body is located near the right vertical wall, a huge cell was formed between circular body and left vertical wall. The flow is very weak between the body and the right vertical wall. Because the body behaves as an obstruction for flow field as seen from Fig. 13e. The isotherms are distributed diagonally from the left bottom corner to the circular body. They again cumulated the top side of the right vertical wall.

Fig. 14 shows the effects of Grashof number on the flow and temperature fields for the location center of body is $c = c$ ($x = 0.5$, $y = 0.5$) and $R = 0.2$. The body is considered as isothermal. For the case of $Gr = 10^5$, a circulation cell is formed at the left top corner of the circular body and a mini cell is formed at the top right corner as given in Fig. 14a. In Fig. 14b, forced convection still becomes effective and the mini cell moves towards to the moving wall. However; Fig. 14c shows that natural convection heat transfer becomes dominant at $Gr = 10^7$. In this case, the flow field becomes more complex and multiple cells were formed. Thus, the isotherms are almost perpendicular to the vertical walls except close to the vertical walls.

Table 3 lists the mean Nusselt number on both cold and hot walls in case of upward moving walls and downward moving walls which makes a comparison for mean Nusselt numbers for different thermal boundary conditions of inserted circular body. The table shows that values of mean Nusselt numbers are equal to each other in the cases of the adiabatic and the conductive thermal boundary conditions of circular body. On the contrary, a higher

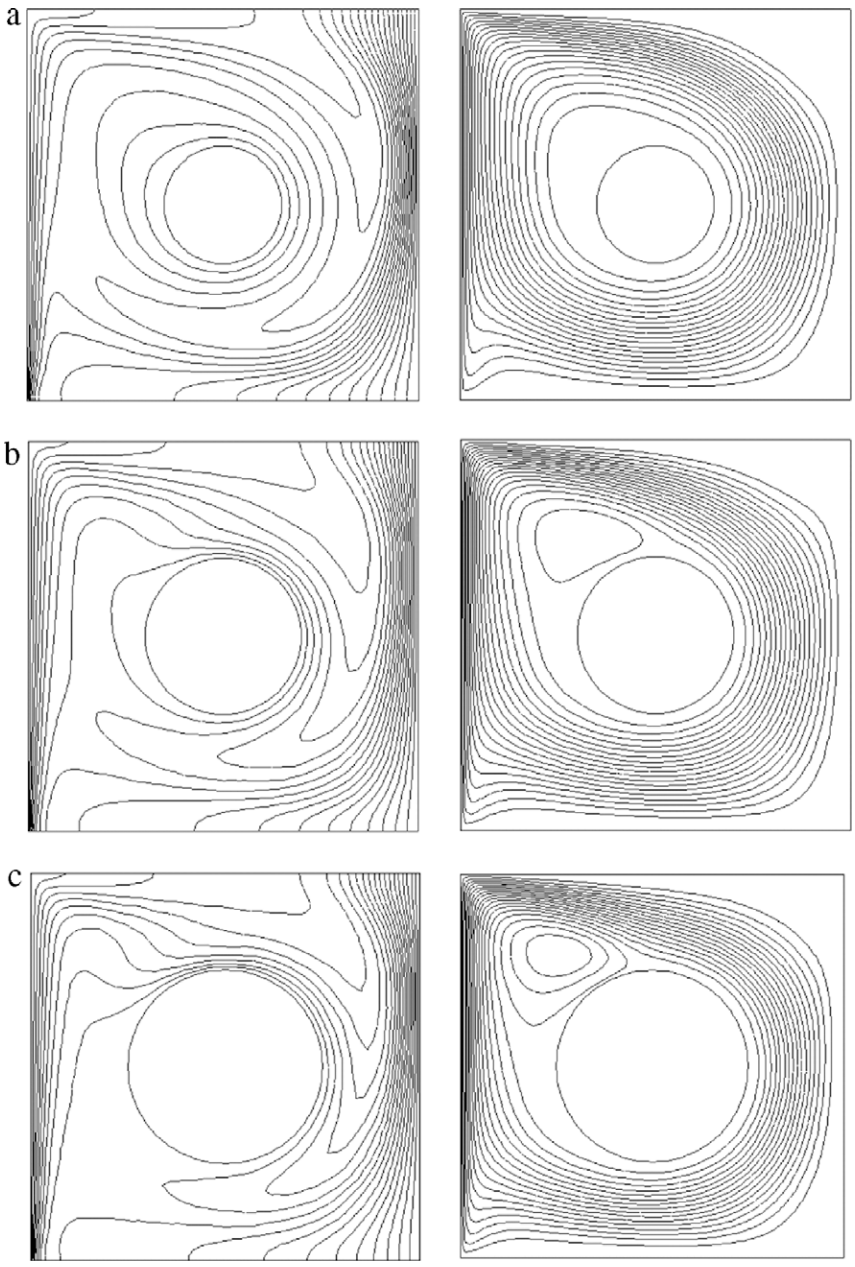

Fig. 12. Isotherms (on the left) and streamlines (on the right) in the case of upward moving walls for isothermal cylinder at different diameter, Gr = 10^5, Pr = 0.71, c = 0.5, and Re = 1000 (a) R = 0.15, (b) R = 0.20 and (c) R = 0.25.

heat transfer is formed on moving wall. Higher heat transfer is formed when lid-driven wall moves in +y direction. Table 4 makes a comparison for mean Nusselt numbers for different thermal boundary conditions of inserted circular body and the different values of the Reynolds number. As shown from the table, heat transfer increases with increasing Reynolds number for all cases. General observation shows that the highest heat transfer is observed for the case of isothermal boundary conditions of circular body as expected. However, an important result is that there is not a big difference between the cases of adiabatic and conductive thermal boundary conditions of circular body. Table 5 gives the effects of location of center of circular body on the heat transfer. The table illustrates that the maximum heat transfer is occurred at hot wall for the coordinates for location center of circular body as x = 0.5 and y = 0.5. On the contrary, when the body locates near the top side as $c = c$ (x = 0.5, y = 0.6), the highest heat transfer is formed on hot wall. Heat transfer increases with increasing Grashof number for constant values of Reynolds number as tabulated in Table 6. Table 7 lists the effects of thermal conductivity on mean Nusselt number. For small diameter of the circular body as R = 0.2, the heat transfer becomes constant. In other words, it is independent from the changes of thermal conductivity ratio. It is noticed that the thermal conductivity ratio is defined as the ratio of thermal conductivity of fluid to solid. Finally, Table 8 lists the average Nusselt numbers for Re = 1000, Gr = 10^5, $c = c$ (x = 0.5, y = 0.5) for *upward* moving wall and isothermal (θ = 0.5). The heat transfer decreases along the cold wall with increasing diameter of the circular body due to decrease of domain of the enclosure. On the contrary, it increases at hot wall with increasing diameter.

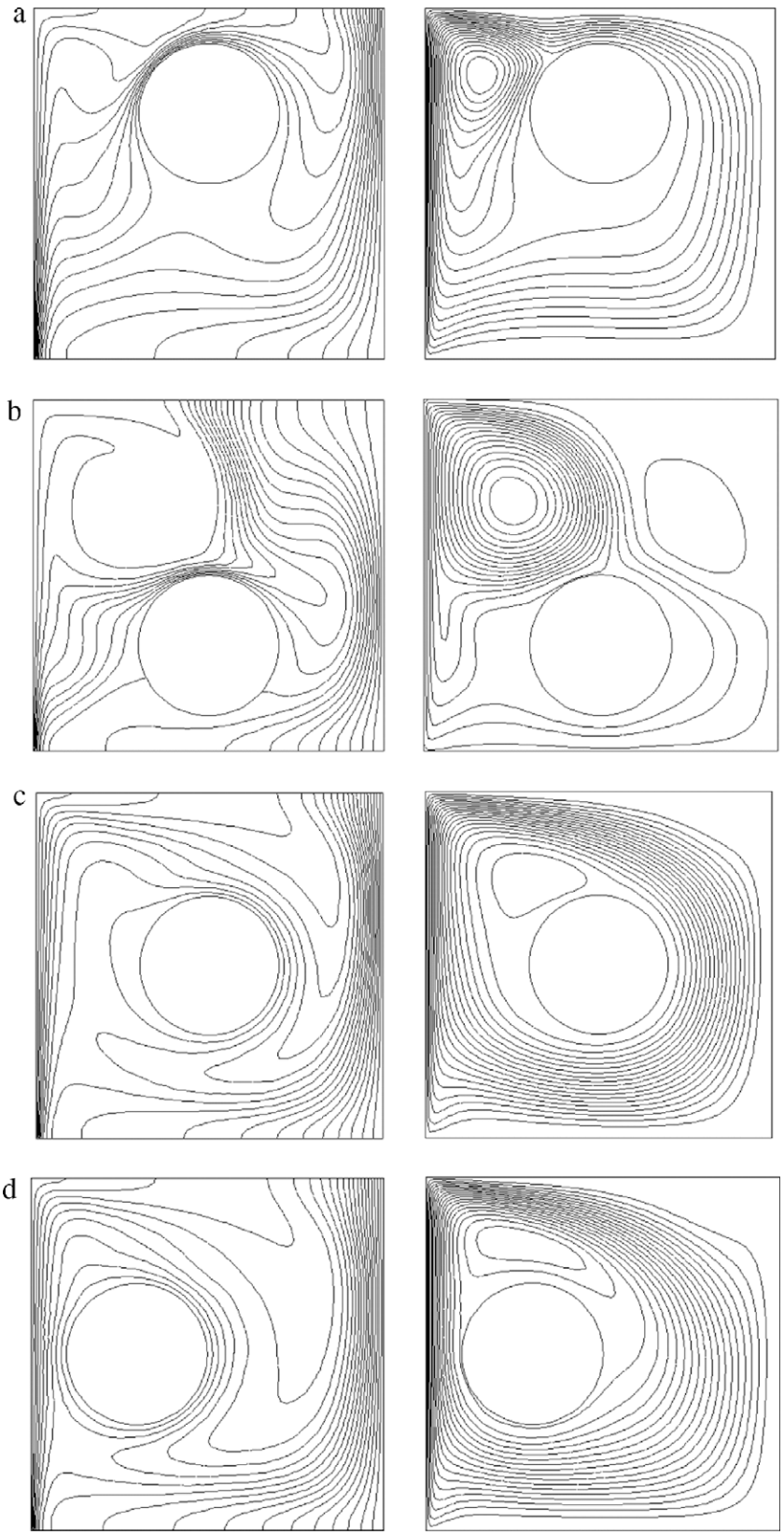

Fig. 13. Isotherms (on the left) and streamlines (on the right) for upward moving lid at different locations of inserted body at $Gr = 10^5$, $Pr = 0.71$, $Re = 1000$, $R = 0.2$, (isothermal cylinder $\theta = 0.5$) (a) $c = c(x = 0.5, y = 0.6)$, (b) $c = c(x = 0.5, y = 0.4)$, (c) $c = c(x = 0.5, y = 0.5)$, (d) $c = c(x = 0.4, y = 0.5)$ and (e) $c = c(x = 0.6, y = 0.5)$.

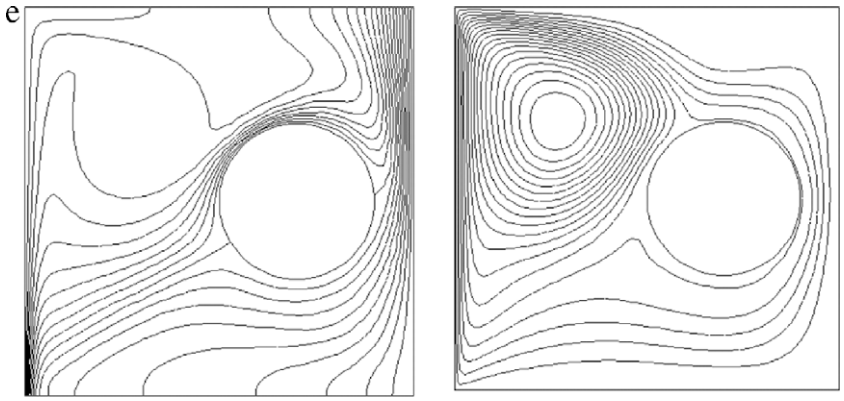

Fig. 13 (*continued*)

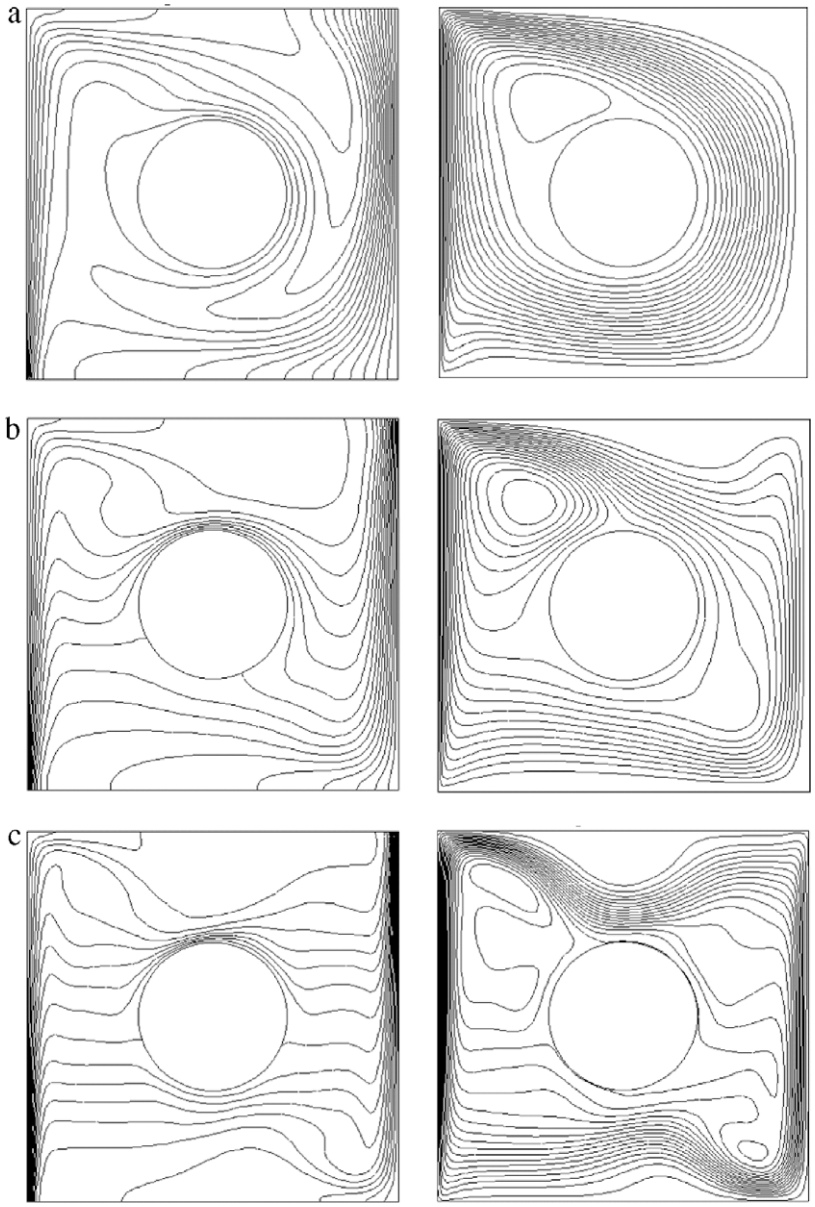

Fig. 14. Isotherms (on the left) and streamlines (on the right) for upward moving lid at higher Grashof number, $c = c(x = 0.5, y = 0.5)$, $R = 0.2$ and $Re = 1000$, in the case of isothermal cylinder ($\theta = 0.5$), (a) $Gr = 10^5$, (b) $Gr = 10^6$ and (c) $Gr = 10^7$.

Table 3
Mean Nusselt numbers for both cases for Re = 1000, Gr = 10^5, $c = c$ ($x = 0.5$, $y = 0.5$) and $R = 0.15$.

	Wall moves upwards		Wall moves downwards	
	Cold wall	Hot wall	Cold wall	Hot wall
Adiabatic	7.88	7.88	5.43	5.43
Conductive	8.08	8.08	5.60	5.60
Isothermal	7.21	9.13	6.04	8.09

Table 4
Comparison of mean Nusselt numbers depends on the cases of circular cylinder for, Gr = 10^5, $c = c$ ($x = 0.5$, $y = 0.5$) and $R = 0.2$ (a) isothermal ($\theta = 0.5$), (b) conductive ($K = 0.001$) and (c) adiabatic.

	The wall moves upwards		The wall moves downwards	
	Cold wall	Hot wall	Cold wall	Hot wall
(a)				
Re = 100	4.60	5.34	3.60	3.06
Re = 500	5.93	8.87	3.44	3.31
Re = 1000	7.14	10.37	6.16	9.39
(b)				
Re = 100	4.96	4.96	3.30	3.30
Re = 500	6.90	6.90	3.37	3.37
Re = 1000	8.12	8.12	6.00	6.00
(c)				
Re = 100	5.24	5.24	3.44	3.44
Re = 500	6.97	6.97	3.51	3.51
Re = 1000	8.11	8.11	6.01	6.01

Table 5
The list of average Nusselt numbers depends on the location of the inserted circle for Re = 1000, Gr = 10^5, $R = 0.2$ for isothermal boundary condition ($\theta = 0.5$) and upward moving wall.

Location center of the body	Hot wall	Cold wall
$c = c(x = 0.5, y = 0.6)$	5.38	11.78
$c = c(x = 0.5, y = 0.4)$	4.00	7.70
$c = c(x = 0.5, y = 0.5)$	7.14	10.37
$c = c(x = 0.4, y = 0.5)$	6.14	10.72
$c = c(x = 0.6, y = 0.5)$	6.65	10.46

Table 6
The list of average Nusselt numbers for different Grashof numbers for Re = 1000, $c = c$ ($x = 0.5$, $y = 0.5$), $R = 0.2$, $\theta = 0.5$ and upward moving wall.

Gr	Cold wall	Hot wall
10^5	7.14	10.37
10^6	10.19	14.21
10^7	17.53	20.50

Table 7
The table of average Nu of all the 20 cases for conductive body (wall moves in $+y$ direction).

Diameter of circular body				
Thermal conductivity	0.2	0.3	0.35	0.4
$K = 0.001$	8.12	8.73	8.58	7.77
$K = 0.1$	8.12	8.82	8.88	8.28
$K = 1$	8.12	8.91	9.27	9.13
$K = 10$	8.12	8.93	9.36	9.38

Table 8
The list of average Nusselt numbers for Re = 1000, Gr = 10^5, $c = c$ ($x = 0.5$, $y = 0.5$) for isothermal inner body (the wall moves in $+y$ direction).

	Cold wall	Hot wall
$R = 0.15$	7.21	9.13
$R = 0.20$	7.14	10.37
$R = 0.25$	6.78	11.10

5. Conclusion

Two-dimensional laminar mixed convection in a circular body inserted lid-driven cavity is investigated numerically for different governing parameters as wide range of Reynolds number, Grashof numbers, center of location and diameter of circular body in this study. Two different orientations are tested for moving wall as $+y$ and $-y$ directions. Based on above discussions the important results can be summarized as:

(a) The circular body can be used as a control parameter for heat transfer, fluid flow and temperature distributions.
(b) Increasing of Grashof number enhances the heat transfer for fixed values of Reynolds number. Heat transfer and fluid flow are strongly affected from the changing of location center of the circular body. Higher heat transfer is formed when the body locates near the top side of the enclosure.
(c) The solution is not sensitive to thermal conductivity for low values of diameter of circular body. But mean Nusselt number increases with increasing of diameter of the inserted body.
(d) Flow field and temperature distribution are affected from the direction of moving wall. Higher heat transfer is observed for the case of downward moving wall. Multiple circulation cells were observed for the downward moving lid in some cases.
(e) Flow field, heat transfer and temperature distribution present different configuration at different thermal boundary conditions of circular body.

Acknowledgement

The authors express their thanks to the reviewers for the valuable comments and suggestions.

References

Angeli, D., Levoni, P., Barozzi, G.S., 2008. Numerical predictions for stable buoyant regimes within a square cavity containing a heated horizontal cylinder. Int. J. Heat Mass Transfer 51, 553–565.
Aydın, O., 1999. Aiding and opposing mechanisms of mixed convection in a shear- and buoyancy-driven cavity. Int. Comm. Heat Mass Transfer 26, 1019–1028.
Bruneau, C.H., Saad, M., 2006. The 2D lid-driven cavity problem revisited. Comput. Fluids 35, 326–348.
Cesini, G., Paroncini, M., Cortella, G., Manzan, M., 1999. Natural convection from a horizontal cylinder in a rectangular cavity. Int. J. Heat Mass Transfer 42, 1801–1811.
Chamkha, A.J., 2002. Hydromagnetic combined convection flow in a vertical lid-driven cavity with internal heat generation or absorption. Num. Heat Transfer Part A 41, 529–546.
Dagtekin, I., Oztop, H.F., 2002. Mixed convection in an enclosure with a vertical heated block located. In: Proceedings of ESDA2002: Sixth Biennial Conference on Engineering Systems Design and Analysis, pp. 1–8.
Dong, S.F., Li, Y.T., 2004. Conjugate of natural convection and conduction in a complicated enclosure. Int. J. Heat Mass Transfer 24, 2233–2239.
FLUENT User's Guide, Fluent Inc., 2002.
Ghia, U., Ghia, K.N., Shin, C.T., 1982. High-Re solutions for incompressible flow using the Navier-Stokes equations and a multigrid method. J. Comp. Phys. 48, 387–411.
Hayase, T., Humphrey, J.A.C., Greif, R., 1992. A consistently formulated QUICK scheme for fast and stable convergence using finite-volume iterative calculation procedure. J. Comp. Phys. 98, 108–118.

Iwatsu, R., Hyun, J.M., 1992. Convection in a differentially-heated square cavity with a torsionally-oscillating lid. Int. J. Heat Mass Transfer 35, 1069–1076.
Iwatsu, R., Hyun, J.M., 1995. Three-dimensional driven-cavity flows with a vertical temperature gradient. Int. J. Heat Mass Transfer 38, 3319–3328.
Iwatsu, R., Hyun, J.M., Kuwahara, K., 1993. Mixed convection in a driven cavity with a stable vertical temperature gradient. Int. J. Heat Mass Transfer 36, 1601–1608.
Jami, M., Mezrhab, A., Bouzidi, M'hamed, Lallemand, P., 2007. Lattice Boltzmann method applied to the laminar natural convection in an enclosure with a heat-generating cylinder conducting body. Int. J. Therm. Sci. 46, 38–47.
Kahveci, K., 2007. Natural convection in a partitioned vertical enclosure heated with a uniform heat flux. J. Heat Transfer 129, 717–726.
Kim, B.S., Lee, D.S., Ha, M.Y., Yoon, H.S., 2007. A numerical study of natural convection in a square enclosure with a circular cylinder at different vertical locations. Int. J. Heat Mass Transfer. doi:10.1016/j.ijheatmasstransfer.2007.06.033.
Mansutti, D., Graziani, G., Piva, R., 1991. A discrete vector potential model for unsteady incompressible viscous flows. J. Comp. Phys. 92, 161–184.
Moallemi, M.K., Jang, K.S., 1992. Prandtl number effects on laminar mixed convection heat transfer in a lid-driven cavity. Int. J. Heat Mass Transfer 35, 1881–1892.
Mohammad, A.A., Viskanta, R., 1993. Flow and thermal structures in a lid-driven cavity heated from below. Fluid Dynam. Res. 12, 173–184.
Oztop, H.F., 2005. Laminar Fluid Flow and Heat Transfer in a lid-driven cavity with rectangular body inserted, 14th Conference on Thermal Engineering and Thermogrammetry, Budapest, Hungary.
Öztop, H.F., Dağtekin, İ., 2001. Laminar flow in a block inserted lid-driven cavity. J. Therm. Sci. 21, 55–63 (In Turkish).
Oztop, H.F., Dagtekin, I., 2004. Mixed convection in two-sided lid-driven differentially heated square cavity. Int. J. Heat Mass Transfer 47, 1761–1769.
Patankar, S.V., 1980. Numerical Heat Transfer and Fluid Flow. Hemisphere, New York.
Shankar, P.N., Despande, M.D., 2000. Fluid mechanics in the driven cavity. Ann. Rev. Fluid Mech. 136, 93–136.
Sharif, M.A.R., 2007. Laminar mixed convection in shallow inclined driven cavities with hot moving lid on top and cooled from bottom. Appl. Therm. Eng. 27, 1036–1042.
Shi, X., Khodadadi, J.M., 2002. Laminar fluid flow and heat transfer in a lid-driven cavity due to a thin fin. J. Heat Transfer 124, 1056–1063.
Shi, X., Khodadadi, J.M., 2004. Fluid flow and heat transfer in a lid-driven cavity due to an oscillating thin fin: transient behavior. J. Heat Transfer 126, 924–930.
Shi, X., Khodadadi, J.M., 2005. Periodic state of fluid flow and heat transfer in a lid-driven cavity due to an oscillating thin fin. Int. J. Heat Mass Transfer 48, 5323–5337.
Torrance, K., Davis, R., Eike, K., Gill, D., Gutman, D., Hsui, A., Lyons, S., Zien, H., 1972. Cavity flows driven by buoyancy and shear. J. Fluid Mech. 51, 221–231.
Varol, Y., Oztop, H.F., Koca, A., 2008. Entropy generation due to conjugate natural convection in enclosures bounded by vertical solid walls with different thicknesses. Int. Comm. Heat Mass Transfer 35, 648–656.